Appendix 3
Momentum Damping from Ion-Neutral Collisions

A3.0: Introduction

Ion-neutral friction represents a potential sink for momentum in a plasma with a significant number of neutrals. To quantify the effect of neutral friction on flow damping, it is necessary to both measure the neutral density and to know the correct rate coefficients for the process. In the course of this research, an extensive study was done of the available atomic data for the proper calculation of the rate coefficients. This appendix discusses the calculation of the rate coefficient for momentum scattering, for collisions with both hydrogen atoms and hydrogen molecules.

In Section 1, the general structure of the problem is laid out, including definitions of the different cross sections and a description of how to include the ion-neutral friction in the fluid equations. Section 2 contains data on cross sections for elastic scattering of protons off of hydrogen atoms and molecules. Section 3 contains calculations of the rate coefficient like quantities $\Omega^{(l,m)}$, which are used to calculate the collision frequencies for momentum scattering. Section 4 contains cross sections and rate coefficients for charge exchange between protons and hydrogen atoms and molecules. Section 5 briefly summarizes the different analytic fits to cross sections and rate coefficients used in the report. Section 6 synthesizes the data and presents a set of conclusions.

A theme throughout this appendix will be the differences in the data between the different sources. Much of the experimental data on cross sections and rate coefficients is subject to 50% or larger error, and many of the calculations have not been properly verified experimentally.

Hence, for any one process, there can be large variations from source to source. This appendix will detail a “best” set of data from the literature for use in analyzing HSX plasmas.

A3.1: Description of the Problem

A3.1.1: Definitions of the Cross Sections.

If a flux of particles I (particles/(area*time)) is incident on a scattering center which deflects the particles, then the number of particles scattered per unit time into an element of solid angle $d\Omega$ is $dn=I\sigma_d(\theta,\varphi)d\Omega$.[1] The factor $\sigma_d(\theta,\varphi)$ is a proportionality factor and is called the differential cross section (DCS). We usually have $\sigma_d(\theta,\varphi)$ independent of φ, so that $\sigma_d(\theta)=2\pi\sigma_d(\theta,\varphi)$. Then the number of particles scattered through an element $d\theta$ at an angle θ is $2\pi I\sigma_d(\theta)\sin(\theta)d\theta$. The total scattering cross section is the integral of $\sigma_d(\theta)$ over all angles. This is given by

$$\sigma^T(V_i) = 2\pi\int_0^\pi \sigma_d(V_i,\theta)\sin(\theta)d\theta, \tag{A3.1}$$

where the possible velocity dependence of the differential cross section is noted. Hence, $\sigma_T I$ is the total number of particles scattered by the beam per unit time into all angles.

The momentum transfer cross section σ_M is related to the DCS by[2]

$$\sigma^M(V_i) = 2\pi\int_0^\pi (1-\cos(\theta))\sigma_d(V_i,\theta)\sin(\theta)d\theta. \tag{A3.2}$$

Note that this heavily weights processes that redirect the motion of the particles ($\theta=\pi$). This cross section is the one of relevance to momentum transport studies involving neutral collisions, as will be shown below.

The integral in the total scattering cross section is known to only converge for potentials that go to zero at finite range.[2] This problem can only be properly treated with a proper quantum mechanical calculation. In the classical calculations, a cutoff angle in the integration is introduced which, in theory, keeps the proper physics but forces the total cross section to a finite value. This

introduction of a cutoff angle can, on the other hand, introduce a degree of arbitrariness in the classical calculation of the total cross section, as will be shown below. The momentum cross section (and higher integral cross sections, see below) are finite for interaction potentials which tend to zero faster than $r^{-1.2}$.

Finally, a general expression for the hierarchy of "integral" cross sections is given by

$$\sigma^{l}(V_i) = \begin{cases} \sigma_T & l = 0 \\ 2\pi \int_0^{\pi} \left(1 - \cos^{l}(\theta)\right) \sigma(V_i, \theta) \sin(\theta) d\theta & l > 0 \end{cases}. \quad \text{(A3.3)}$$

A3.1.2: Derivation of the Elastic Scattering Term in the Fluid Equations.

The general need is to understand how to represent the ion-neutral friction term in the momentum balance equation. In the following discussion, the variable **v** will refer to the total velocity, with **u** representing the average velocity and **w** the random velocity. As is shown in[3], the **v** moment of the Boltzman equation yields a momentum equation of the form for particles of species a

$$m_\alpha n_\alpha \left(\frac{d\mathbf{U}_\alpha}{dt} + \mathbf{U}_\alpha \cdot \nabla \mathbf{U}_\alpha \right) = Z_\alpha e n_\alpha \left(\mathbf{E} + \frac{\mathbf{U}_\alpha \times \mathbf{B}}{c} \right) - \nabla p_\alpha - \nabla \cdot \Pi_\alpha + m_\alpha n_\alpha \frac{\delta \mathbf{U}_\alpha}{\delta t}. \quad \text{(A3.4)}$$

The last term in this equation represents change in the fluid element's momentum due to all collisions, and the proper collision physics must be involved in this term. For elastic collisions between species a and b, it is possible to simplify the final term as:

$$m_\alpha n_\alpha \frac{\delta \mathbf{U}_\alpha}{\delta t} = -m_{\alpha\beta} n_\alpha \left(\mathbf{U}_\alpha - \mathbf{U}_\beta \right) \bar{\upsilon}_{\alpha\beta}. \quad \text{(A3.5)}$$

In this expression, $m_{\alpha\beta}=m_\alpha m_\beta/(m_\alpha+m_\beta)$ is the standard reduced mass, and $\nu_{\alpha\beta}$ is an effective collision strength for momentum transfer. In this case, the damping is proportional to the reduced mass and the relative average velocity of the two species. The collision strength can be written as

$$\bar{\upsilon}_{\alpha\beta} = \frac{1}{3}\sqrt{\frac{2}{\pi}} \left(\frac{m_{\alpha\beta}}{T_{\alpha\beta}} \right)^{5/2} n_\beta \int_0^{\infty} w^5 \sigma^{M}(w) \exp\left(-\frac{m_{\alpha\beta}}{2T_{\alpha\beta}} w^2 \right) dw. \quad \text{(A3.6)}$$

In this expression, $T_{\alpha\beta}=(m_\beta T_\alpha+m_\alpha T_\beta)/(m_\beta+m_\alpha)$ is an effective temperature, and the integration is over the random relative velocities ($\mathbf{w}=\mathbf{w}_\alpha-\mathbf{w}_\beta$).

This integral is related to the $\Omega^{(l,m)}$ integrals of classical gas transport [1,2]. These integrals are defined as

$$\Omega^{(l,r)}\left(T_{\alpha\beta}\right)=\frac{a_{\alpha\beta}}{2\sqrt{\pi}}\int_0^\infty d\xi e^{-\xi^2}\xi^{2r+1}\sigma^l(T_{\alpha\beta}\xi^2), \tag{A3.7}$$

where $\xi=v_r/a_{\alpha\beta}$, and $a_{\alpha\beta}=(2T_{\alpha\beta}/m_{\alpha\beta})^{1/2}$. Note that $T_{\alpha\beta}\xi^2$ is simply the collision energy in the CM frame. These $\Omega^{(l,r)}$ integrals are tabulated for various collision processes of interest in [2], or can be numerically calculated from any source of the appropriate cross section (σ^T for $\Omega^{(0,0)}$, σ^M for $\Omega^{(1,1)}$, etc.). It is then possible to write the effective collision frequency for momentum transport as

$$\overline{\upsilon}_{\alpha\beta}=\frac{16}{3}n_\beta\Omega^{(1,1)}. \tag{A3.8}$$

This expression shows that the Ω integrals have units of cm^3/s, which are the standard units for rate coefficients. It is apparent that (16/3) $\Omega^{(1,1)}$ acts as a rate coefficient for momentum transfer collisions. Further, it can be shown that the rate coefficient for *all* collisions is related to $\Omega^{(0,0)}$ as [2]:

$$<\sigma v>=8\Omega^{(0,0)}. \tag{A3.9}$$

It should be noted that the effective collision frequencies in Golant et .al. and Bachmann et. al. are the same, when a proper transformation of integration variables is used. The definition of effective temperature is equivalent in the two references. As can be seen, the problem of momentum damping is reduced to the evaluation of the effective collision strength for momentum transfer, which requires an integration of the momentum transfer cross section over the relative velocity between the two species. Data for the momentum transfer cross sections and Ω integrals will be presented in sections 2 and 3.

A3.1.3: The Charge Exchange Term in the Fluid Equations.

Charge exchange is a second process that can damp the momentum of ions in the plasma, and will be shown to be the dominant process for protons interacting with atomic hydrogen. This damping mechanism is often discussed in the context of the L-H transition, where it can damp flows and inhibit H-mode access. For instance fluid modeling of the TEXTOR biased H-mode has been done with an ion-neutral friction term of the form $n_i m_i \nu_{i0} \mathbf{U}_i$.[4] The collision frequency is simply the charge exchange frequency

$$\upsilon_{i0} = n_n < \sigma_{CX} v_i > . \qquad \text{(A3.10)}$$

This modeling appear to be much more heuristic than the formal derivation presented for the case of pure elastic scattering. Formally, this expression is the rate at which charge exchange collisions occur, not the rate at which momentum is transferred from one species to another. The difference between these two rates is determined by the distribution of angles of the charge exchanged ions, as accounted for by 1-cos(θ) weighting in σ^M. This topic will be developed fully in Section 2.2. It will be shown that a proper quantum mechanical calculation for proton-hydrogen atom collision will include both "elastic scattering" and charge exchange in a single formulation. No such unifying calculation exists for hydrogen molecules, and a momentum damping rate from charge exchange of the form in A3.10 will be used.

A3.2: Cross Section Data for Different Elastic Processes.

A3.2.1: Sources

The total and momentum transfer cross sections for protons scattering off of atoms and molecules have been tabulated in a number of references. In the paper by Bachmann and Reiter, a classical calculation is used to calculate the cross-sections for elastic scattering on both atoms and molecules. The results are fit to a function of the form

$$\ln\left(\sigma^{T,M}(E_i)\right) \approx \sum_{n=0}^{3} a_{ln}^{T,M} \ln\left(E_i\right)^n , \quad E_i < E_{i,min} , \qquad \text{(A3.11a)}$$

$$\ln\left(\sigma^{T,M}(E_i)\right) \approx \sum_{n=0}^{8} a_n^{T,M} \ln(E_i)^n, \quad E_{i,min} < E_{i,min} < E_{i,max} . \tag{A3.11b}$$

$$\ln\left(\sigma^{T,M}(E_i)\right) \approx \sum_{n=0}^{3} a_{rn}^{T,M} \ln(E_i)^n, \quad E_{i,max} < E_i . \tag{A3.11c}$$

In these expressions, a_n, a_{ln}, a_{rn}, $E_{i,min}$, and $E_{i,max}$ are parameters given for each type of collision, and are available in both their paper on the internet.[5] The energies E_i in the formula are in the lab frame, with the assumption that the neutral is still. Hence, the energy in the center of mass frame is given by $E_{cm}=(m_r/m_i)E_i$. Note that their paper contains some errors in the fit coefficients, so it is highly recommended that the values from the web site are used.

Krstic and Schultz[6] give a comprehensive account of elastic scattering cross sections for all isotopes of hydrogen. The calculations are done using full quantum mechanical models. Data is presented for both the differential cross sections and the integral cross sections, in both tabular form and with numerical fits. In particular, the integral cross sections are fit to a function of the form:

$$\sigma^{t,m}(E) = 2.80028 \times 10^{-17} \frac{\sum_{i=0} a_i (\ln(E))^i}{1 + \sum_{j=1} b_i (\ln(E))^i} (cm^2) . \tag{A3.12}$$

In this reference, all energies E are in the CM frame. The fit parameters a_i and b_i are provided in their paper, and the tabular data is available on the Internet[7] as well as in their paper[6].

A3.2.2: Proton Elastic Scattering off of Hydrogen Molecules.

Other less complete sources exist for the case of protons colliding with hydrogen molecules. The fit to momentum transfer cross section in Tabata[8] is based on the data by Phelps[9]. The data for σ_M in Phelps is not a first principle calculation, but is based on a small amount of data which is extrapolated based on physics assumptions to form a complete set of

recommended data. The data on the total scattering cross section in the early work by Barnett[10] is taken from Cramer[11]. Note that the presented by Cramer need to be divided by 3.536×10^{16} cm^3 to compare them with the calculations. A fully quantum mechanical calculation has been done by Baer et. al.[12] at a CM energy of 20 eV.

The total cross section for the $p+H_2$ elastic scattering is shown in figure A3.1, for all the sources from which data is available.

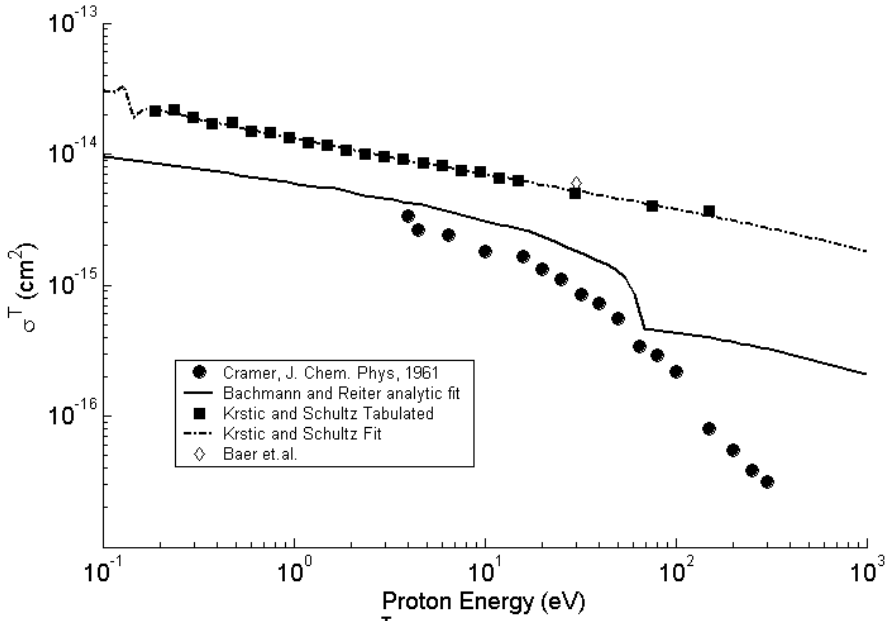

Figure A3.1: σ^T for $p+H_2$ elastic scattering.

The data for the total cross section shows fairly poor agreement between the two sources. According to Krstic and Schultz, the error in the Bachmann calculation is partly related to an improper choice of the deflection cutoff. The quantum mechanical calculation by Baer agrees closely with the Krstic and Schultz result. The old data by Cramer falls under all the theoretical calculations.

Fortunately, the disagreement in the total cross section is unimportant; the momentum transfer cross section is the quantity which enters into transport calculations. The data on this important cross section is shown in figure A3.2.

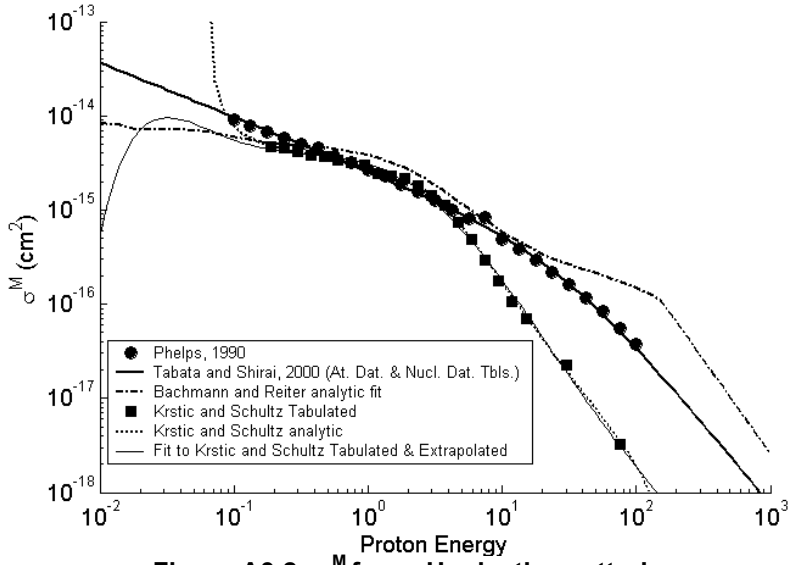

Figure A3.2: σ^M for p+H_2 elastic scattering.

The different sources generally agree well for impact energies less than 30 eV. Above that energy, the fully quantum mechanical calculations deviate significantly from the other two sources. The data recommended by Phelps and the calculations by Bachmann are in fairly close agreement. Unfortunately, the data in the Phelps recommendation is based on experimental data only up to 2.3 eV. In Phelps' paper, he notes that his momentum cross section is lower by an order of magnitude than one calculation, and specifically states that more theory and experiment are needed for 1eV<E<1keV. The fit by Tabata smoothly interpolates the data from Phelps, although that paper also provides some warning about the momentum cross section above 1eV. Krstic and Schultz note that vibrational motion of the molecule will cause a decline in the momentum transfer cross section above 10 eV, an effect not considered in the classical calculation. Given the uncertainty and lack of data, indications are that the Krstic and Schultz data are the most trustworthy[13], and they will be the primary source for this reaction in the future.

In the Section 3.1, the $\Omega^{(1,1)}$ integrals will be numerically integrated for the different models of the momentum transfer cross section. The analytic fit provided by Krstic and Schultz has bad properties outside the range .1 eV<E_r<100 eV, making the integration over particle energies difficult. To fix this, the tabulated data have been smoothly extrapolated outside the

range of the tabulated data and fit to a polynomial. The fit is shown in A3.2, and the fit parameters are provided in Section A3.5.

A3.2.3: Proton Elastic Scattering off of Hydrogen Atoms.

The works by Bachmann and Reiter and by Krstic and Schultz contain calculated cross section data for the elastic scattering of protons off of atomic hydrogen. In the work by Bachmann and Reiter, a purely classical model of the scattering process is invoked. This has limitations, especially at low energies. For the case of H^++H, quantum mechanical effects become important. In particular, the two nuclei should be regarded as indistinguishable at low energy, and a proper quantum mechanical calculation is needed to resolve this physics.

The fully quantum mechanical calculation by Krstic reveals many new features. In these calculations, the key physics point is the inability to distinguish between a slow proton elastically scattered off of the atom from the slow proton resulting from the charge exchange event. The two processes are indistinguishable. As the energy increases, the overlap in the two channels is reduced and the differential cross section shows the classical separation of a forward peak (scattering) and backward peak (charge exchange). Throughout the work by Krstic, the combination of these two channels is maintained, so that the "elastic" differential cross section contains the effects of both resonant charge exchange and classical elastic scattering.

In the calculations, it is possible to distinguish between the two particles by labeling them by there spin. In this case, it is possible to distinguish between the "spin-exchanged" particles and the scattered particles. In the high energy limit, the spin exchange cross section becomes the standard charge-exchange cross section. This distinction allows the calculation of the traditional elastic cross section. Quoting their paper: "*The "true elastic" differential cross sections may be approximated as the absolute value of the difference of the presented "elastic" and charge transfer differential cross sections. This can then be used to recalculate the integral quantities, such as momentum transfer and viscosity cross sections to obtain results that have the right*

classical limits…the spin exchange cross section defined in the low energy limit goes smoothly over to the proper charge transfer cross section in the classical limit of distinguishability." This section will demonstrate that by using the appropriately calculated quantum mechanical DCS from Krstic and Shultz data, the more traditional and familiar results regarding charge exchange and classical elastic scattering can be reproduced.

The techniques described above for separating the effects of charge exchange and classical elastic scattering require the knowledge of the DCS. In the Krstic and Schultz reference, the DCS has been fit to an analytic function, with the fit parameters provided in their paper. Alternatively, the raw data is available in tabular form on the internet. The quantities $2\pi\sin(\theta)\sigma_{d,el}(\theta,E)$ for elastic scattering and $2\pi\sin(\theta)\sigma_{d,se}(\theta,E)$ for charge exchange are tabulated for 768 angles between 0 and π, for 30 CM collision energies between .1eV and 100eV. Unfortunately, the fits only approximate the structure of the DCS; for all subsequent calculations, interpolation in the tabulated DCS will be used.

Krstic and Schultz also provide a table of integral cross section data corresponding to calculations done in the indistinguishable (IP) and (DP) sense, The DP calculation is based on a DCS which is weighted toward forward scattering, and is to be used in situations where elastic scattering and charge exchange are treated as separate processes. The IP data is used in cases where the two processes can be combined.

Figure A3.3 displays the different DCS for a CM energy of .1 eV.

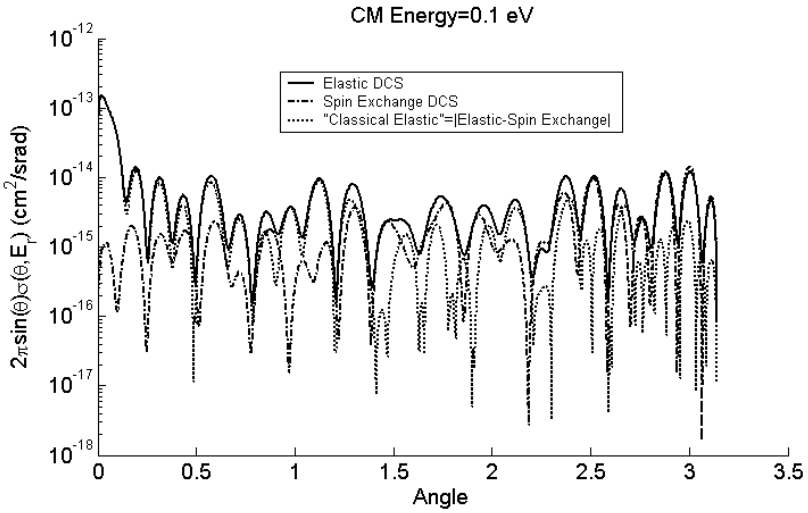

Figure A3.3: DCS for p+H scattering at E_{cm}=.1eV.

These graphs show that at low CM energy, there is no strong peak for either forward or backward scattering. Hence, there is little separation of the classical elastic (forward) scattering channel and the charge exchange (backward scattering) channels.

The equivalent plot for a CM energy of 100 eV is shown in figure A3.4. At high energy, there are clear peaks for forward scattering (traditional elastic scattering in this limit) and backward scattering (traditional charge exchange). The 1-cos(θ) weighting in the momentum transfer cross section largely eliminates the large peak at forward angles in the calculation of σ^M. This leads to the conclusion that the charge exchange channel will dominate the momentum transfer process.

With these differential scattering cross sections, it is possible to proceed to the integral cross sections. Because the total cross section is technically divergent for a classical calculation, it is necessary to introduce a cutoff angle in the integration to keep the cross section finite. This cutoff can lead to a total cross section with little physical meaning, while the quantum mechanical cross section still has the meaning described by equation (A3.1). Hence, it is not worthwhile to compare the classical and quantum mechanical calculations of the total cross section.

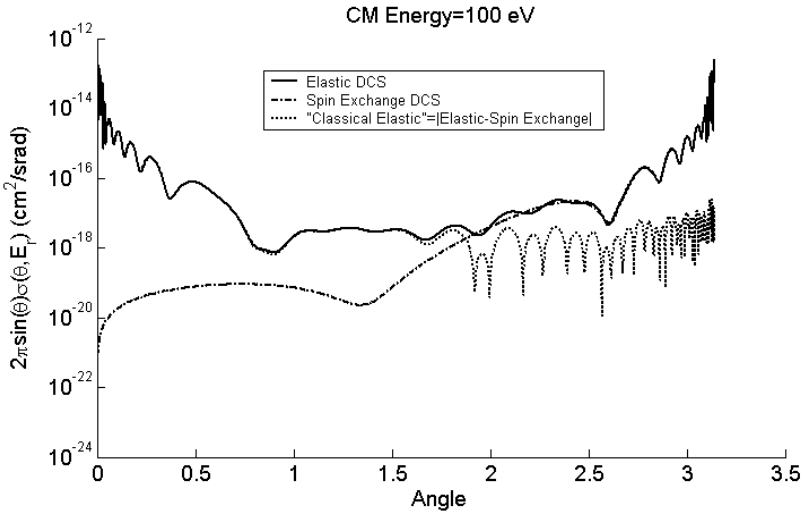

Figure A3.4: DCS for p+H scattering at E_{cm}=100eV.

The momentum cross section is finite in both sets of calculations, and is shown in Figure A3.5, using both classical and quantum mechanical calculations of σ^M. The two analytic fits (classical and quantum mechanical calculations) show very different trends as a function of proton energy. The discrepancy can be understood as follows. The Bachmann result includes only elastic scattering in the distinguishable particle sense; i.e. no charge exchange. The appropriate quantum mechanical calculation for comparison for this process comes from using the "classical elastic" DCS when computing σ^M. The σ^M calculated this was is surprisingly close to the Bachman result. Note also that the tabulated Krstic and Schultz "distinguishable particle" (DP) approximation agrees closely with the Bachmann and Reiter result.

As the proton energy is increased, the classical elastic scattering contribution to σ^M becomes less important compared to the charge exchange component. This confirms the traditional result that charge transfer is the dominant process for momentum loss in ion-atom interactions. In section 4, more traditional data for charge exchange cross sections and rate coefficients will be presented, allowing further comparisons with the quantum mechanical calculation. These results are already sufficient to demonstrate that the quantum mechanical calculations of Krstic and Schultz are the preferred way of treating all processes in p+H collisions.

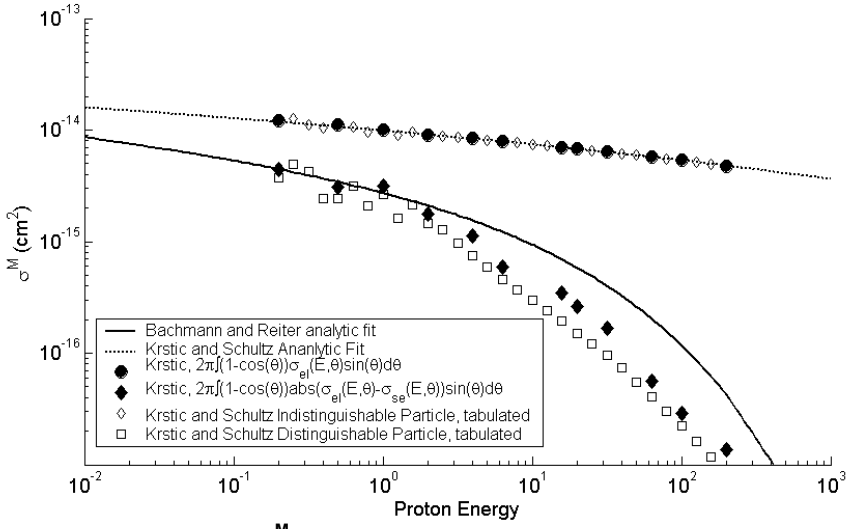

Figure A3.5: σ^M vs. proton energy for p+H collisions.

A3.3: The Integrals $\Omega^{(l,r)}$

A3.3.1: Protons Scattering on Molecular Hydrogen (p+H_2).

The integral quantity $\Omega^{(1,1)}$ is tabulated as a function of ion energy in reference Bachmann and Reiter, based on their classical calculations. In this case, the fit to the data is specified as

$$\ln\left(\Omega^{(1,1)}\left(T_{\alpha\beta}\right)\right) \approx \sum_{n=0}^{8} a_n^{1,1} \ln\left(T_{\alpha\beta}\right)^n , \tag{A3.13}$$

where $T_{\alpha\beta}$ is the effective temperature defined earlier. The values of $\Omega^{(1,1)}$ are based on the momentum transfer cross sections calculated in that reference using classical techniques, not experimental data.

The little direct experimental data comes from experiments in drift tube mass spectrometer to measure the mobility of trace ions in a background gas. The mobility is defined as the ratio of the static drift velocity (v_d) of the ions to the electric field (E) accelerating them:

$$v_d = KE . \tag{A3.14}$$

It is possible to show[14] that

$$v_d = q\frac{E}{N}\frac{3}{8}\sqrt{\frac{\pi}{2m_r T_{eff}}}\frac{1}{\omega^{(1,1)}}. \tag{A3.15}$$

The drift velocity is proportional to E, as the electric field specifies the acceleration of the proton between collisions. The drift velocity is inversely proportional to the number density of background molecules (N), as these molecules lead to collisions which retard the movement of the protons. In this expression, T_{eff} is an effective temperature defined as

$$\frac{3}{2}k_B T_{eff} = \frac{3}{2}k_B T + \frac{1}{2}m_i v_d^2, \tag{A3.16}$$

and the new collision integral, $\omega^{(1,1)}$, is related to the previous $\Omega^{(1,1)}$ as

$$\Omega^{(1,1)} = \sqrt{\frac{T_{eff}}{2\pi m_r}}\omega^{(1,1)}. \tag{A3.17}$$

In these equations, T is the temperature of the background gas in the drift tube, and m_r is the reduced mass as specified before. In comparing the two forms of the collision integral T_{eff} and $T_{\alpha\beta}$ have been made set equal to each other. Note that for clarity in this document, the notation has been changed slightly from the notation in Ellis, et. al.[15], where $\omega^{(1,1)}$ is confusing called $\Omega^{(1,1)}$.

The experimental values of v_d, $\omega^{(1,1)}$, and T_{eff} are provided for many different combinations of ions and background gasses Ellis, et. al. The data relevant for this study is a table for the scattering of protons in a background of hydrogen molecules. The data is provided in terms of $\omega^{(1,1)}$, which is transformed to $\Omega^{(1,1)}$ as described above. T_{eff} and $T_{\alpha\beta}$ are used interchangeably in the transformation.

Using the definition of the integral $\Omega^{(1,1)}$, it is possible to numerically integrate this quantity from any tabulation of the momentum transfer cross section. This enables $\Omega^{(1,1)}$ for a given calculation of σ^M to be checked against limited available experimental data. In doing this integration, it is important to be sure that the analytic form of the momentum cross section is valid for the entire range of energies included in the integration. For the calculation shown here, the

integration was done over a range of energies $T_{eff}/25<E<25T_{eff.}$ The total of experimental data, analytic fits, and numerically calculations are shown in figure A3.6.

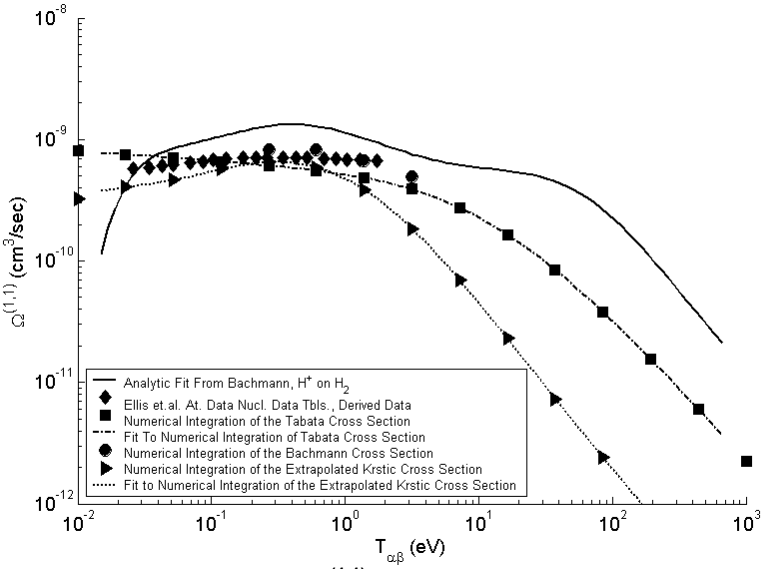

Figure A3.6: $\Omega^{(1,1)}$ for p+H_2 collisions.

The analytic form of Bachmann is slightly above the experimental data from Ellis. The values of $\Omega^{(1,1)}$ numerically integrated from the Tabata and Shirai σ^M or the Krstic and Schultz σ^M agree very well with the available data. At higher temperatures, the Bachmann and Reiter analytic form is the largest, with the Krstic form the smallest. This is due to the fall of in the Krstic σ^M for energies above 10eV. The $\Omega^{(1,1)}$ values calculated from the Tabata and Shirai σ^M appear to split the difference between the other calculations. Never the less, the data from Krstic and Schultz appear to be the most creditable, and the $\Omega^{(1,1)}$ calculated with their data will be used as the reference case. Note that the numerically integrated $\Omega^{(1,1)}$ data have been fit to analytic functions. These fits are shown in A3.6, and are listed in table A3.1.

A3.3.2: Protons Scattering on Atomic Hydrogen.

The Ω integrals for the p+H collisions are calculated in the same way as for the p+H_2 process. The important difference is that, as discussed above, this calculation includes important

effects in the coupling of elastic scattering and charge transfer. The analytic fit to $\Omega^{(1,1)}$ from Bachmann and Reiter and the numerical integrated values are shown in the figure A3.7.

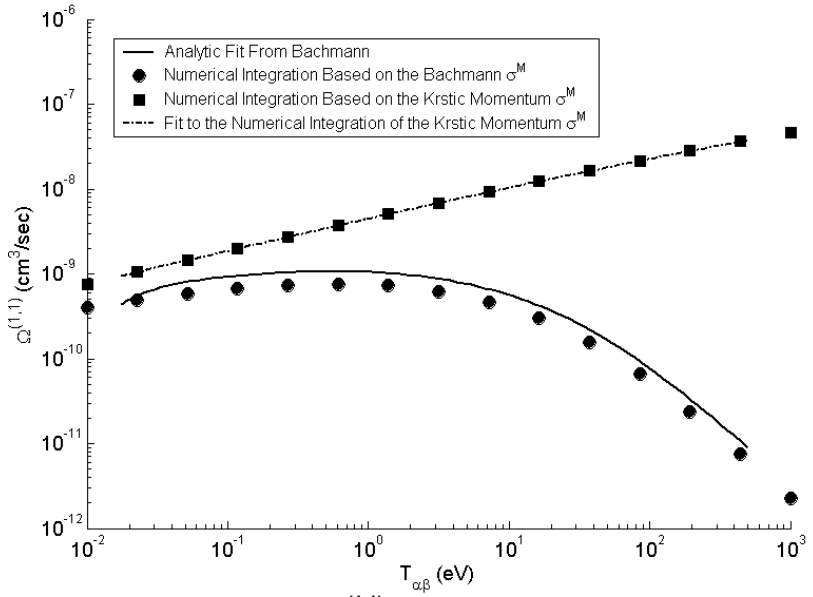

Figure A3.7: $\Omega^{(1,1)}$ for p+H collisions.

As noted repeatedly above, the difference between these curves is the consistent inclusion of charge exchange effects in the case of the Krstic and Schultz calculation. The analytic fit parameters for the Krstic and Schultz fit is given in table A3.2

A3.4: Charge Exchange Cross Sections and Rate Coefficients.

Besides elastic scattering, charge exchange must be considered as a sink for momentum. Large amounts of data are in existence for the cross sections for protons charge exchanging with atoms and molecules. Unfortunately, most of the data in the literature is for proton impact energies above 1keV. This is the energy range relevant to energetic neutral beam interactions, but is beyond the energies of thermal ions in HSX.

A3.4.1: Charge Exchange between Protons and Hydrogen Molecules.

The cross section for $p+H_2$ collisions has been calculated and tabulated in a number of sources. Sources of raw data for different energies include the papers by Barnett[10], Gealy and Van Zyl[16], and Koopman.[17] The analytic fit by Tabata and Shirai[8] is based on the recommended data in Phelps.[9] Analytic fits by Freeman and Jones[18] and Janeev[19] provide a simply means of interpolating the data. The fit by Janeev is stated to be an interpolation for 15 eV<E_r<50 eV. The results from these sources are shown in figure A3.8.

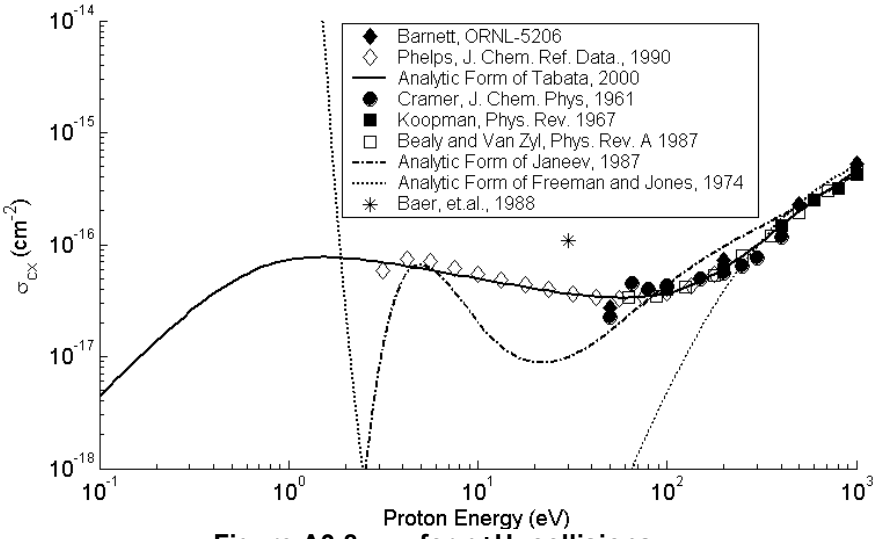

Figure A3.8: σ_{cx} for $p+H_2$ collisions.

As can be seen from the plot, the Janeev does not fit the data well in the energy range where it was interpolated. The analytic fit by Freeman and Jones is good at only high impact energy and fails spectacularly for E<100 eV. The fit by Tabata appears to fit the data most accurately, although this conclusion is based solely on the assumption that the Phelps recommended data are correct for E<30 eV. It is clear that the charge exchange rate for $p+H_2$ collisions is not well established for E<100eV. The theoretical calculation by Baer et. al. appears to be slightly above the other data.

The rate coefficient for charge exchange between protons and hydrogen molecules has been fit to an analytic form by Freeman and Jones,[18] based on the analytic fit to the rate

coefficient. Note that there is a misprint in this article: there should be a logarithm on both sides of their polynomial fit in section three of the introduction. For comparison, analytic cross section of Freeman & Jones[18], Tabata[8], and, Janeev[19] have been numerically integrated against a Maxwellian distribution. The integration was done over particles with energy $T_i/100<E<100T_i$. Based on the above cross sections, it is anticipated that the Freeman and Jones rate coefficient will only be valid for $T_i>100$ eV. The rate coefficients based on the Tabata and Janeev fits are expected to be more accurate at low energies. These analytic and numeric rate coefficients are shown in figure A3.9.

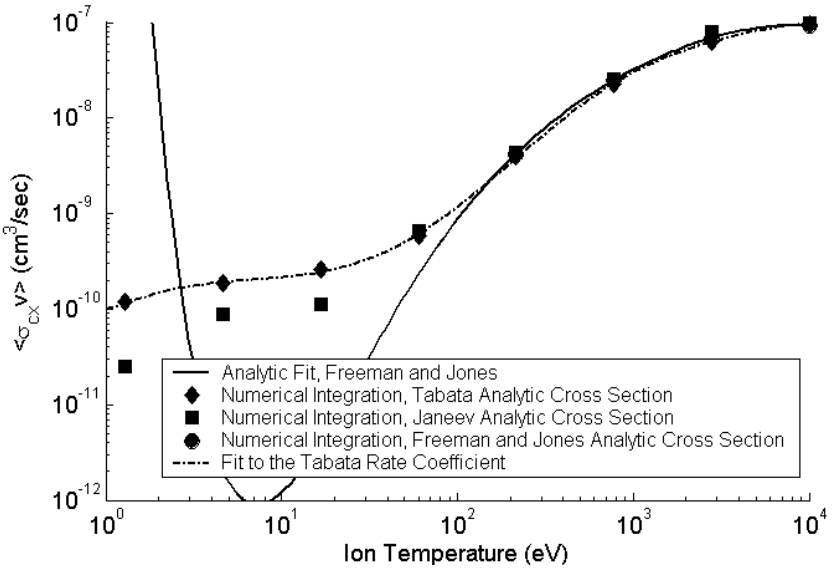

Figure A3.9: $<\sigma_{cx}v>$ for $p+H_2$ collisions.

It is obvious that when the Freeman and Jones analytic cross section is numerically integrated to calculate a rate coefficient, it agrees with the Freeman and Jones analytic rate coefficient. This testifies to the consistency of that data set. For $T_i<80$ eV, the Freeman and Jones rate coefficient is significantly less than the numerically derived values from Janeev and Tabata, and in not considered reliable by the author of this report. The dip in the Janeev cross section at 20eV is seen to bring the rate coefficient down compared to the Tabata value for low temperatures.

Based on all of this data, the numerically integrated rate coefficient based on the Tabata cross section appears to be the most reliable. This rate coefficient has been fit as discussed in section A3.5. The fit parameters are provided in table A3.1, and the quality of the fit is shown in figure A3.9.

A3.4.2: Charge Exchange between Protons and Hydrogen Atoms.

A great deal of data exists for the cross section for charge exchange between protons and atomic hydrogen, although most of it is at higher energy. Freeman and Jones provide a simple formula for the cross section:

$$\sigma_{cx,H} = \frac{.6937\times10^{-14}\left(1-0.155\log_{10}(E)\right)^2}{1+.1112\times10^{-14}E^{3.3}}(cm^2). \qquad (A3.18)$$

The data from Barnett[20] is provided in tabulated form. The experimental data in Newman, et. al.[21] and Gealy & Van Zyl[16], is provided in tabular forms with error bars. The data in Tawara et al.[22] and Fite et al.[23] is mostly at higher energies, and must be read off a graph to determine values. The process of reading the data off of the graph introduces some error in the graph below. The book by Janeev[19] provides a simple analytic form of this cross section. Figure A3.10 illustrates the good agreement between the data sets.

The analytic form of Freeman and Jones and Janeev appears to fit the data from many sources well, although it may be slightly high. Further, this expression extrapolates well to low energies. The analytic form by Janeev also fits the data well, but does not extrapolate well to low energies. This will be important when evaluating rate coefficients. The IP spin exchange cross section from Krstic and Schultz[6] tends to sit in the scatter of the experimental data, lending confidence to that quantum mechanical calculation.

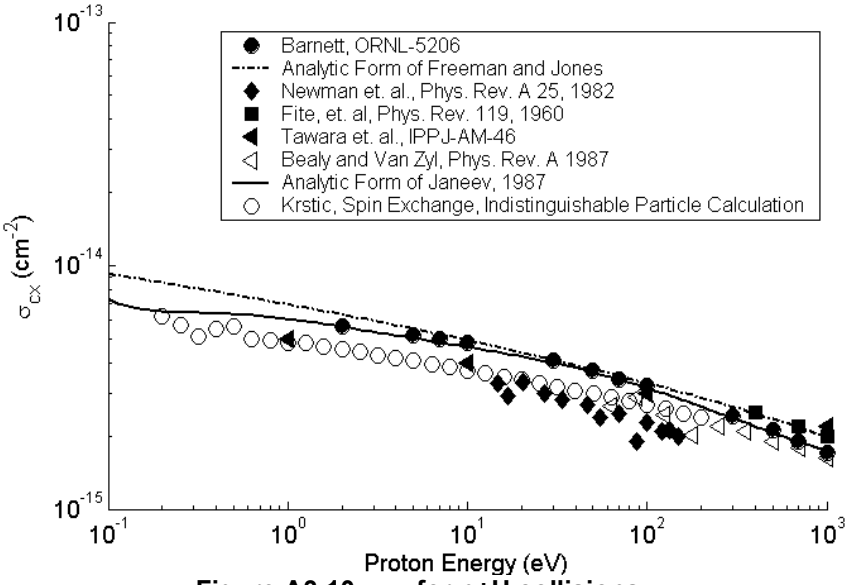

Figure A3.10: σ_{cx} for p+H collisions.

The final quantity to discuss is the rate coefficient for proton-atom charge exchange. In the paper by Cornelis[21], the rate coefficient is given as

$$< \sigma_{cx} v >= 10^{-8} T_i^{.318} . \qquad \text{(A3.19)}$$

No range of applicability is given for the fit. The analytic fit by Freeman and Jones is stated to be good in the energy range of 1eV to 100keV. In addition, the cross sections from Freeman and Jones and from Janeev were numerically integrated to derive the rate coefficient. The integration was done for $T_i/100<E<100T_i$. For $T_i<1$eV, this integration could fail, due to the poor behavior of the cross section analytic forms at low energy. The various calculations of the p+H rate coefficient are shown in figure A3.11.

Based on this data, the analytic fit by Freeman and Jones has been selected as the appropriate means to represent the proton-atom charge exchange rate coefficient. This data appears to be questionable for ion temperatures below 1eV, which is the stated lower limit of the analytic forms applicability.

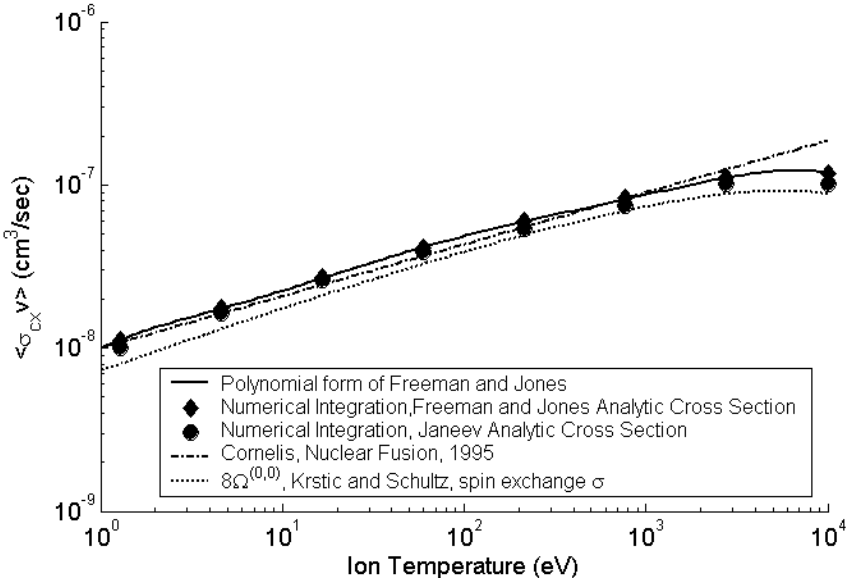

Figure A3.11: $<\sigma_{cx}v>$ for p+H collisions.

As a final point of comparison, it was stated in Section A3.1.2 that the rate coefficient for a process is given by $8\Omega^{(0,0)}$. In section A3.2.3, it was shown that the quantum mechanical calculation of elastic scattering for the p+H_2 reaction includes a spin exchange term that becomes the traditional charge exchange process above about 1eV. Hence the rate coefficient for charge exchange calculated in this section should be equal to the quantity $8\Omega^{(0,0)}$, where the spin exchange DCS is used to calculate σ^T in the calculation of $\Omega^{(0,0)}$. Figure A3.11 shows the excellent agreement between these quantities and lends confidence to the entire formalism.

A3.5: Summary of Analytic Fits.

Many rate coefficients, cross sections, and Ω integrals have been fit in this report. All of them have been fit to a function of the form

$$\ln(f) \approx \sum_{n=0}^{8} a_n \ln(x)^n . \qquad \text{(A3.20)}$$

In this expression, f could represent Ω, σ, or $<\sigma v>$, and x could represent T_i, T_{eff}, E_i or E_r, The table below provides the fit parameters for these fits. In no cases have the fits been tested to the accuracy of those found in the refereed literature.

Parameters	1. Krstic and Schultz σ^M, p+H_2, extended	2.Tabata and Shirai $\Omega^{(1,1)}$, p+H_2	3. Krstic and Schultz $\Omega^{(1,1)}$, p+H_2,	4.Tabata and Shirai $<\sigma v>_{cx}$, p+H_2
a_0	-33.6453	-21.2924	-21.3742	-22.985057
a_1	-0.70536	-0.16951	-0.553961	.6694131359
a_2	-0.354471	-0.0504561	-0.248971	-.1875214003
a_3	-0.0364058	-0.013732	0.00563185	$-.246949x10^{-1}$
a_4	0.0205793	-0.00052472	0.00813684	$.10649315.x10^{-1}$
a_5	0.000327074	0.000357204	-0.00073384	$.58798933x10^{-2}$
a_6	-0.000561123	9.73171e-006	-0.000115252	$-.191458651x10^{-2}$
a_7	4.47933e-005	-5.18618e-006	2.19459e-005	$.189237109x10^{-3}$
a_8	-5.65137e-007	2.08049e-007	-1.10458e-006	$-.628954476x10^{-5}$
Independent Variable	E_{cm}	T_{eff}	T_{eff}	T_i

Table A3.1: Fits for p+H_2 collision processes

Parameters	1. Krstic and Schultz $\Omega^{(1,1)}$, p+H	2. Krstic and Schultz $\Omega^{(0,0)}$, p+H, based on spin exchange σ
a_0	-19.2219	-20.5518
a_1	0.372866	0.387916
a_2	-0.000137784	-0.00505016
a_3	-.000137784	-0.000338638
a_4	-4.94137e-006	-3.13511e-005
a_5	-1.46294e-007	-2.92195e-006
a_6	-6.29297e-009	1.84907e-007
a_7	1.78525e-010	1.81937e-009
a_8	-3.98841e-008	-1.00575e-008
independent Variable	T_{eff}	T_{eff}

Table A3.2: Fits for p+H collision processes

A3.6: Synthesis of the Data Presented in the Appendix.

For p+H collisions, all of the classical elastic scattering and charge exchange physics are encapsulated in the Krstic and Schultz indistinguishable particle calculations. For p+H collisions where no such combination is possible, the two processes have to be taken separately. The calculations chosen to represent the two processes are shown in figure A3.12.

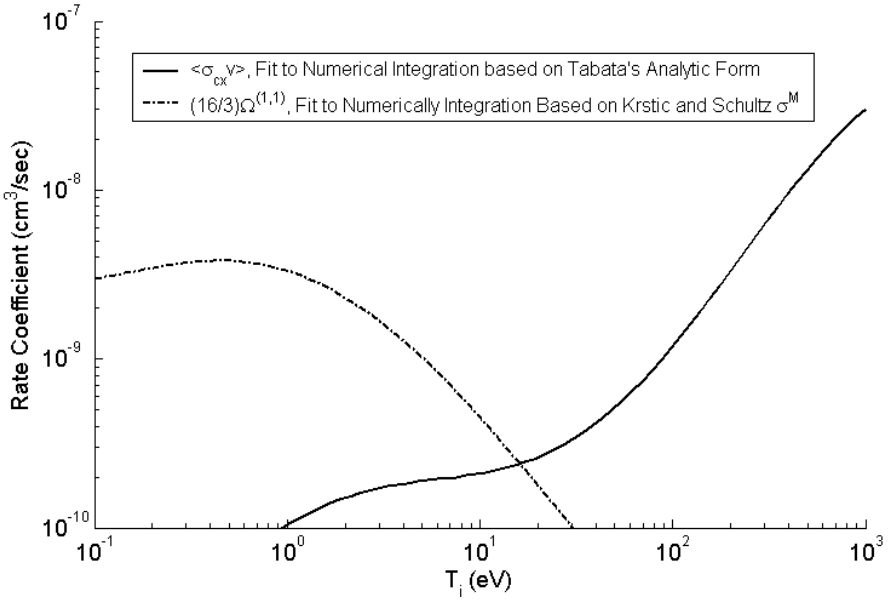

Figure A3.12: Comparison of the competing processes for p+H_2 collisions.

In the ion temperature range of HSX (T_i=25 eV), charge exchange seems to be the dominant process. Note that, as discussed before, the treatment of charge exchange here is not on par with the treatment of elastic scattering, and should be taken as an estimate only.

In the model by Coronado and Talmadge,[24] the formulation upon which the modeling in this paper is based, the ion neutral collision term is written as $m_i n_i \nu_{in} U_i$. In writing this, we assume that the neutrals are at rest in the lab frame. Equating this to the terms given above yields:

$$m_i n_i \upsilon_{in} U_i = m_{pH} n_i \overline{\upsilon}_{pH} U_i + m_{pH_2} n_i \overline{\upsilon}_{pH_2} U_i + m_i n_i n_{H_2} \left\langle \sigma_{cx,H_2} v \right\rangle U_i . \qquad \text{(A3.21)}$$

The velocity and ion density can be factored out and the appropriate terms involving $\Omega^{(1,1)}$ inserted to yield:

$$\upsilon_{in} = \frac{16}{3}\frac{m_{pH}}{m_i} n_H \Omega_{pH}^{(1,1)} + \frac{16}{3}\frac{m_{pH_2}}{m_i} n_{H_2} \Omega_{pH_2}^{(1,1)} + n_{H_2} \left\langle \sigma_{cx,H_2} v \right\rangle . \qquad \text{(A3.22)}$$

Consider a plasma with a neutral hydrogen density of $1x10^{10}$ cm^{-3} and a molecular hydrogen density of $1x10^{10}$ cm^{-3}. These numbers are approximately those given by three dimensional DEGAS simulations of HSX plasmas. The individual contributions to the collision frequency and the sum of the three terms are plotted in figure A3.13.

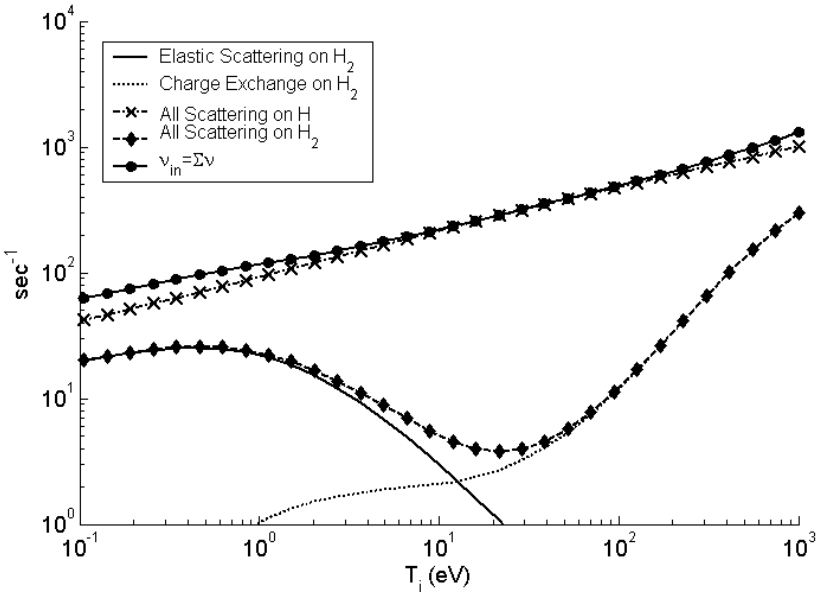

Figure A3.13: Ion-neutral collision frequencies.

It is clear that for this case, the elastic scattering of protons on H dominates the momentum damping process at HSX relevant temperatures; collisions with molecules can be virtually ignored.

[1] F. J. Blatt, *Modern Physics*, (McGraw-Hill, New York, 1992).

[2] P. Bachmann and D. Reiter, Contrib. Plasma. Phys. **35**, 45 (1995).

[3] V. E. Golant, A.P. Zhilinsky, I. E Sakharov, and S. C. Brown, *Fundamentals of Plasma Physics*, (John Wiley & Sons, New York, 1977).

[4] J. Cornelis, R. Sporken, G. Van Oost, and R.R. Weynants, Nuclear Fusion **34**, 171 (1994).

[5] www.eirene.de

[6] P.S. Krstic and D.R. Schultz, Atomic and Plasma-Material Data for Fusion **8**, 1 (1998).

[7] http://www-cfadc.phy.ornl.gov/elastic/homeh.html

[8] T. Tabata and T. Shirai, Atomic Data and Nuclear Data Tables **76**, 1 (2000).

[9] A.V. Phelps, J. Phys. Chem, Ref. Data **19**, 653 (1990).

[10] C.F Barnett et. al., ORNL Report 3113, Oak Ridge National Laboratory, 1963.

[11] W.H. Cramer, J. Chem. Phys. **35**, 836 (1961).

[12] M. Baer, G. Niedner, and J.P. Poennies, J. Chem. Phys. **88**, 1461 (1988).

[13] Private communication, Detlev Reiter.

[14] E.W. McDaniel and E. A. Mason, *The Mobility and Diffusion of Ions in Gases*, (John Wiley & Sons, New York, 1973).

[15] H. W. Ellis, R.Y. Pai, E.W. McDaniel, E.A. Mason, and L.A. Viehland, Atomic Data and Nuclear Data Tables **17**, 177 (1976).

[16] M. W. Gealy and B. Van Zyl, Phys. Rev. A **36**, 3091 (1987).

[17] D. W. Koopman, Physical Review **154**, 79 (1967).

[18] R. L. Freeman and E. M. Jones, CLM-R 137, UKAEA Research Group 1974.

[19] R. K. Janeev, W.D. Langer, K. Evans, Jr., D. E. Post, Jr., *Elementary Processes in Hydrogen-Helium Plasmas* (Springer, Berlin, 1987).

[20] C.F Barnett, J.A. Ray, E. Ricci, M.I. Wilker, E. W. McDaniel, E.W Thomas, and H. B. Gilbody, ORNL Report 5206, Oak Ridge National Laboratory, 1977.

[21] J. H. Newmann, J.D. Cogan, D.L. Viegler, D. E. Nitz, R.D. Rundel, K.A. Smith, and R. F. Stebbings, Physical Review A **25**, 2976 (1982).

[22] H. Tawara, Y. Itikawa, Y. Itoh, T. Kato, H Nishimura, S Ohtani, H. Takagi, K. Takayanagi, and M. Yoshinko, Report IPPJ-AM-46, Institute of Plasma Physics, Nagoya University.

[23] W. L. Fite, R. F. Stebbings, D. G. Hummer, and R. T. Brackmann, Physical Review **119**, 663 (1960).

[24] M. Coranado and J. N. Talmadge, Phys. Fluids B **5**, 1200 (1993).